Journal of Applied Mechanics and Technical Physics, Vol. 49, No. 2, pp. 157–166, 2008

LINEAR STABILITY OF THREE-DIMENSIONAL BOUNDARY LAYERS

S. A. Gaponov and B. V. Smorodskii

UDC 532.526

Stability of compressible three-dimensional boundary layers on a swept wing model is studied within the framework of the linear theory. The analysis based on the approximation of local self-similarity of the mean flow was performed within the Falkner–Skan–Cooke solution extended to compressible flows. The calculated characteristics of stability for a subsonic boundary layer are found to agree well with the measured results. In the case of a supersonic boundary layer, the results calculated for a Mach number $\mathrm{M} = 2$ *are also in good agreement with the measured spanwise scales of nonstationary vortices of the secondary flow. The calculated growth rates of disturbances, however, are substantially different from the measured values. This difference can be attributed to a high initial amplitude of disturbances generated in the experiment, which does not allow the linear stability theory to be applied. The evolution of natural disturbances with moderate amplitudes is fairly well predicted by the theory. The effect of compressibility on crossflow instability modes is demonstrated to be insignificant.*

Key words: *three-dimensional boundary layer, hydrodynamic stability, laminar–turbulent transition.*

INTRODUCTION

The problem of turbulence emergence in a three-dimensional boundary layer on a swept wing is now intensely studied because of its academic and applied importance. In boundary-layer flows, the laminar–turbulent transition may occur owing to amplification of unstable natural oscillations of the boundary layer. Under comparatively weak external forcing (free-stream turbulence, surface vibrations, or external acoustics), a large part of the laminar–turbulent transition zone is described by the linear theory of hydrodynamic stability.

The research of swept-wing boundary-layer stability was reviewed in [1, 2]. The latest results in this field are summarized in [3]. It is known at the moment that the three-dimensional boundary layer on a swept wing is subjected to hydrodynamic instability of several types; each of them is characterized by its own mode and has its own source of excitation. One of the most important types is the crossflow instability responsible for the early emergence of turbulence on a swept wing. Most results concerning this type of instability were obtained for subsonic velocities. Theoretical research of stability of a compressible three-dimensional boundary layer was started in [4, 5].

The experiments [6] showed that the distribution of the mean and fluctuating characteristics in the boundary layer at supersonic velocities is the same as that at subsonic velocities. Natural fluctuations enhance in the downstream direction.

A method of passive control of the laminar–turbulent transition on supersonic swept wings was found. It was demonstrated in experiments [7, 8] that the use of artificial microscale roughness periodic in the spanwise direction and located near the leading edge of the wing allows the transition to be slightly delayed and shifted in the downstream direction. It is reasonable to use the linear stability theory in choosing the parameters of the process (see [7]).

Khristianovich Institute of Theoretical and Applied Mechanics, Siberian Division, Russian Academy of Sciences, Novosibirsk 630090; gaponov@itam.nsc.ru; smorodsk@itam.nsc.ru. Translated from Prikladnaya Mekhanika i Tekhnicheskaya Fizika, Vol. 49, No. 2, pp. 3–14, March–April, 2008. Original article submitted May 21, 2007.

0021-8944/08/4902-0157

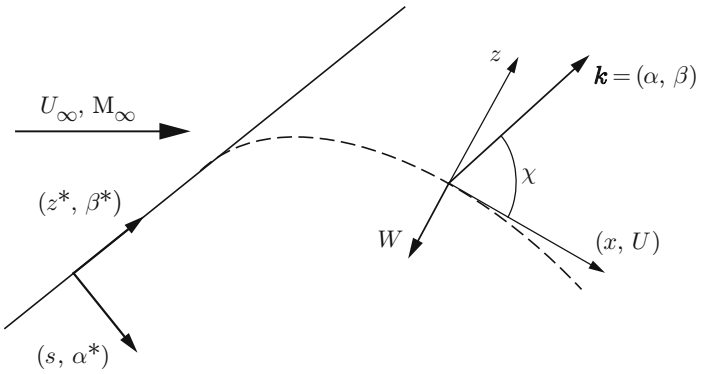

Fig. 1. Geometry of the swept wing and coordinate systems used: the dashed curve is the streamline; the secondary flow velocity is indicated by W.

Experimental investigations of stability of three-dimensional supersonic boundary layers are now undertaken [6, 9, 10]. To analyze and interpret the experimental data, they have to be compared with the results calculated by the linear theory. Such calculations are also necessary to plan experiments on transition control, as it was done in [7].

The present paper describes a theoretical study of linear crossflow instability to stationary and traveling low-amplitude perturbations. A quantitative comparison of theoretical results with experiments conducted at a low subsonic velocity [11] and in a supersonic flow [10] is performed.

1. FORMULATION OF THE PROBLEM

Considering the flow in the boundary layer on an infinite-span swept wing model and its stability, one can reasonably use two commonly accepted coordinate systems (Fig. 1). The system (s, z^*) is fitted to the model (the origin is on the leading edge of the wing). The s axis is directed along the chord over the model contour, and the z^* axis is directed over the wing span parallel to the leading edge. This coordinate system is used to calculate the mean flow characteristics, because its parameters are independent of z^*. It is more convenient, however, to calculate the stability characteristics in a local coordinate system (x, z), where the x axis is directed along the local velocity vector of the potential flow on the boundary-layer edge. In all coordinate systems mentioned, the y axis is aligned normal to the model surface.

1.1. Analysis of Linear Stability. Within the framework of the linear stability problem, we can present the flow field in a compressible boundary layer as a sum of the mean flow and a small perturbation:

$$\boldsymbol{u} = U_\infty(\boldsymbol{U}(x, y) + \varepsilon \boldsymbol{V}(x, y, z, t)). \tag{1}$$

Here the mean flow velocity $\boldsymbol{U}(x, y) = (U(x, y), 0, 0)$ is considered in the approximation of local parallelism, $\varepsilon \boldsymbol{V} = \varepsilon(u, v, w)$ are the components of the velocity disturbance, and $\varepsilon \ll 1$ is a small parameter characterizing the disturbance amplitude. The expressions for the temperature T, pressure P, and density ρ are written in a manner similar to Eq. (1). The equations for disturbances are obtained by substituting Eq. (1) into the Navier–Stokes equations and into the continuity and energy equations. In the present work, we consider a three-dimensional problem of stability, where the frequency is assumed to be a real quantity, and the streamwise wavenumber is assumed to be a complex quantity. An analysis of stability of the boundary-layer flow on a swept wing in the locally parallel approximation usually involves the assumption that the amplitude of localized disturbances increases in the external flow direction x, and disturbances periodic in terms of z^* are amplified along the chord s [12]. The location of the neutral stability curves is independent of the direction of growth of disturbances. Following [12], we assume that the direction of growth of all disturbances coincides with the direction of the external flow streamline. The solution of the problem is presented as

$$\boldsymbol{q} = A(x)\boldsymbol{\varphi}(y) \exp\Big(i \int\limits_{x_0}^{x} \alpha(x')\, dx' + i\beta z - i\omega t\Big),$$

where $\boldsymbol{k} = (\alpha, \beta)$ is the wave vector consisting of the streamwise wavenumber α and spanwise wavenumber β, $\omega = 2\pi f$ (f is the frequency), and the sought vector $\boldsymbol{\varphi}$ is presented as

$$\boldsymbol{\varphi} = (u, v, w, p, \theta)^{\mathrm{t}}, \tag{2}$$

i.e., it consists of three components of the velocity disturbance, pressure disturbance, and temperature disturbance, whereas the disturbances of density and mass flux A are expressed via the components of the vector $\boldsymbol{\varphi}$. In Eq. (2), all quantities are normalized to appropriate parameters of the mean flow outside the boundary layer. In the first approximation in terms of ε, we obtain the linear boundary-value problem

$$\frac{d\boldsymbol{\varphi}}{dy} = H\boldsymbol{\varphi}; \tag{3}$$

$$y = 0: \quad (u, v, w, \theta) = 0, \qquad y \to \infty: \qquad |\boldsymbol{\varphi}| < \infty, \tag{4}$$

where H is the linear operator generalizing the Lees–Lin operator to the case of a three-dimensional boundary layer. The nonzero elements of H taken from [1] depend both on the mean flow properties (velocity and temperature profiles, Mach number M, Reynolds number Re, and Prandtl number Pr) and on the wave parameters (frequency and wavenumbers). The homogeneous boundary conditions (4) are satisfied only under certain combinations of these parameters, which have to be found. Thus, Eqs. (3) and (4) form an eigenvalue problem.

Stability of the flows under considerations was analyzed in the present work by means of numerical integration of system (3), (4) by the method of orthonormalizations [13]. The streamwise wavenumber $\alpha = \alpha_r + i\alpha_i$ was found as the eigenvalue of the boundary-value problem, and the components of the vector $\boldsymbol{\varphi}$ are the corresponding eigenfunctions. The conditions $-\alpha_i > 0$ and $-\alpha_i \leqslant 0$ refer to unstable disturbances amplified in the downstream direction and to stable waves decaying with increasing x.

1.2. Mean Flow. A three-dimensional boundary layer on an infinite-span swept wing can be theoretically described in the approximation of the so-called local self-similarity [14]. Within such a model, the boundary-layer equations are reduced to a system of ordinary differential equations by introducing the Dorodnitsyn–Lees variables, depending on the local Mach number M_e and on the streamwise pressure gradient of the inviscid external flow outside the boundary layer:

$$\xi = \int_0^s \rho_e \mu_e U_e \, ds, \qquad \eta = \frac{\rho_e U_e}{\sqrt{2\xi}} \int_0^y \frac{\rho}{\rho_e} \, dy$$

[U_e is the streamwise (along s) velocity component outside the boundary layer and μ_e is the viscosity]. Assuming that the mean flow parameters are independent of z^*, we can present the stream function, the streamwise and spanwise components of velocity, and enthalpy in the form

$$\psi(s, \eta) = \Phi(s) f(\eta), \quad U(s, \eta) = U_e(s) f'(\eta), \quad W(s, \eta) = W_e(s) q(\eta), \quad I(s, \eta) = I_e(s) g(\eta),$$

where the prime means the derivative with respect to the coordinate η normal to the model surface. Then, in the approximation of local self-similarity, we obtain a system that describes the flow in a three-dimensional boundary layer:

$$\begin{gathered} (Cf'')' + ff'' + [\rho_e/\rho - (f')^2]\beta_H = 0, \qquad (Cq')' + fq' = 0, \\ \left(\frac{C}{\mathrm{Pr}}\, g'\right)' + fg' = \frac{1 - \mathrm{Pr}}{\mathrm{Pr}} \, \frac{(\gamma - 1)\mathrm{M}^2}{1 + (\gamma - 1)\mathrm{M}^2/2} \, [C(f' f'' \cos^2 \lambda_e + qq' \sin^2 \lambda_e)]. \end{gathered} \tag{5}$$

Here λ_e is the local sweep angle, i.e., the angle between the axis s and the local direction of the external flow velocity U_p, γ is the ratio of specific heats, $C = \rho\mu/(\rho_e \mu_e)$, and $\beta_H = (2\xi/U_e)\, dU_e/d\xi$. System (5) is derived under the assumption that the parameters β_H and M_e are independent of the streamwise coordinate ξ. If these parameters depend only weakly on ξ, system (5) has to be applied locally, and its solutions (f, q, g) should be considered as parametrically dependent on the streamwise coordinate.

If there is no boundary-layer suction on the surface, the boundary conditions for a thermally insulated model can be written as

$$\eta = 0: \quad (f, f', q, g') = 0, \qquad \eta \to \infty: \quad (f', q, g) \to 1. \tag{6}$$

System (5) is the generalization of the Falkner–Skan–Cooke equations to the case of a compressible boundary layer flow. In the present work, system (5), (6) was numerically integrated by the fourth-order Runge–Kutta method. The shooting method was used to satisfy the boundary conditions.

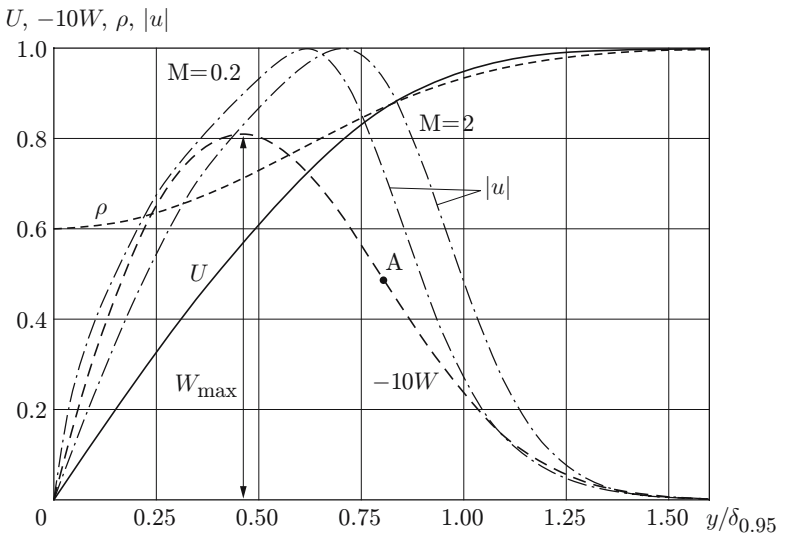

Fig. 2. Mean flow parameters for $M_e = 2$ and fluctuations of streamwise velocity of the stationary ($\omega = 0$) crossflow instability mode for $\beta = 1.3$ and $Re = 5000$.

2. RESULTS OF SIMULATIONS

2.1. Stability of the Self-Similar Boundary Layer. The mean flow and stability were calculated for $Pr = 0.72$ and $\gamma = 1.4$. Some results calculated for stationary ($f = 0$) crossflow instability modes in subsonic and supersonic three-dimensional boundary layers are presented further below.

Figure 2 shows the calculated distributions normal to the model surface for the mean streamwise velocity $U = U(y)$, secondary crossflow velocity $W(y)$, and density $\rho = 1/T$ for $M_e = 2$ (the local values of U, W, and ρ are normalized to the corresponding values outside the boundary layer). The normal coordinate is brought to dimensionless form on the basis of the boundary-layer thickness $\delta_{0.95}$: $U|_{y=\delta_{0.95}} = 0.95U_e$. For chosen parameters, the changes in the mean density inside the boundary layer stays within 40%. The favorable pressure gradient ($\beta_H > 0$) typical of the initial part of the swept wing (closer to the leading edge) is responsible for the formation of a spanwise flow with $W(y) < 0$. The profile $W(y)$ acquires an inflection (point A in Fig. 2), which leads to substantial destabilization of the flow. The most important parameter characterizing instability of the three-dimensional boundary layer considered is the amplitude of the secondary flow $W_{\max}$. In the present case, the secondary flow with $W_{\max} \approx 0.08$ was obtained for $\lambda = 45^\circ$ and $\beta_H \approx 0.29$.

The dot-and-dashed curves in Fig. 2 show the profiles of fluctuations of the streamwise velocity $|u(y)|$ (normalized to the maximum values) at $M_e = 2.0$ and 0.2. The difference in these functions for subsonic and supersonic flow regimes is insignificant and is manifested only in a small shift of the location of the maximum of fluctuations, which correlates well with the shift of the inflection point on $W(y)$.

We calculated the diagram of stability for stationary modes of crossflow instability for $M_e = 2$ and $W_{\max} = -0.08$, i.e., the contours of spatial growth rates on the plane (Re, k_r) ($k_r = \sqrt{\alpha_r + \beta}$ is the absolute value of the wave vector and $Re = \rho_e U_e \delta_{0.95}/\mu_e$ is the Reynolds number). The location of the boundary of the instability region ($-\alpha_i > 0$) is consistent with the results calculated in [12]. For $Re > 3000$, the region of instability becomes almost symmetric with respect to the line of the maximum growth rates. The critical Reynolds number is $Re_{cr} \approx 680$. The calculations showed that the critical Reynolds number decreases with increasing $W_{\max}$, and the values of unstable wavenumbers already for $W_{\max} \geqslant 0.04$ stay within the range $0 < k_r < 3$, which is almost independent of Re and M. According to [12], this is a typical feature of the natural mode of inviscid crossflow instability manifested in the "inflected" profile of the secondary flow. It should be noted that the amplitude of stationary modes cannot increase if there is no secondary flow (in a two-dimensional boundary layer).

The calculated stability diagram for stationary modes showed that the Mach number M exerts only a weak effect on the location and size of the instability region and on the magnitude of the growth rates. In particular,

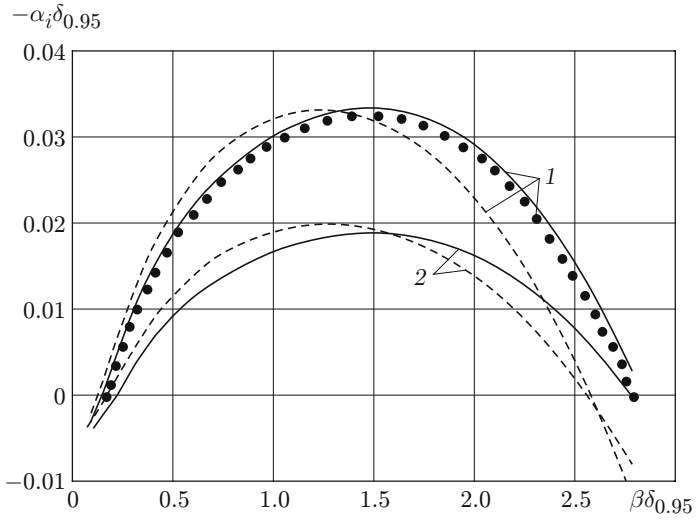

Fig. 3. Spatial growth rates of stationary modes for Re = 5000: curves 1 and 2 refer to $W_{\max} = -0.08$ and -0.05, respectively; the solid and dashed curves show the data for $M_e = 2$ and 0.2, respectively; the points are the results calculated in [12].

for $M_e = 0.2$, the values of Re_{cr} are only 10% lower than for $M_e = 2$. Figure 3 shows the spatial growth rates of stationary modes for $W_{\max} = -0.08$ and -0.05 for Mach numbers $M_e = 2.0$ and 0.2 and Re = 5000. The results of [12] agree well with the data calculated in the present work. With increasing $|W_{\max}|$, the instability is seen to increase, and the influence of compressibility is very small and leads only to a minor shift of the maximum of growth rates whose values for $M_e = 2.0$ and 0.2 differ by less than 10%. The wave vectors of increasing disturbances are aligned almost normal to the inviscid external flow.

2.2. Simulation of Test Conditions in the Subsonic Flow Regime. Gaponenko et al. [11] experimentally studied the linear stage of crossflow instability evolution in a subsonic flow. In the initial cross sections of the swept wing, the mean flow was simulated with the use of a flat plate with an induced favorable pressure gradient. The flat plate was mounted in the wind-tunnel test section at a sweep angle $\lambda = 25°$. The pressure gradient was generated by a dummy wall placed into the test section. The experiments were performed in a T-324 low-turbulence wind tunnel based at the Khristianovich Institute of Theoretical and Applied Mechanics of the Siberian Division of the Russian Academy of Sciences. The flow field in the boundary layer was recorded by a hot-wore anemometer. The crossflow instability modes were artificially excited in the boundary layer by various generators of disturbances operating at frequencies $f = 8.3$, 25.0, and 35.0 Hz. The characteristics of stability of normal modes were obtained by a frequency-wave spectral analysis.

The conditions of the present linear stability calculations were the same as those used in the experiments of [11]. The following parameters obtained in the experiments were used: velocity at the boundary-layer edge $U_e \approx 6.8$ m/sec, displacement thickness $\delta_1 \approx 1.25$ mm, Hartree parameter $\delta_H \approx 0.47$, and Reynolds number $Re_{\delta_1} \approx 560$.

Figure 4 shows the calculated and measured spatial growth rates of normal crossflow instability modes as functions of the spanwise wavenumbers for $f = 35$ Hz. As $W(y) < 0$, the values $\beta > 0$ refer to waves propagating in the direction almost opposite to the secondary flow; for $\beta < 0$, the direction of disturbance propagation coincides with the secondary flow direction. The flow parameters were chosen in experiments to obtain moderate growth rates for all frequencies (to prevent amplification of uncontrolled background disturbances). The calculations predicted that the boundary layer is stable for all values of β. The large scatter of points in Fig. 4 appears because the experimental data on growth rates of disturbances were obtained by means of numerical differentiation of the measured disturbance spectra with respect to the streamwise coordinate, which is responsible for a large error in the final results. With allowance for this fact, the calculated data are in reasonable agreement with the test results.

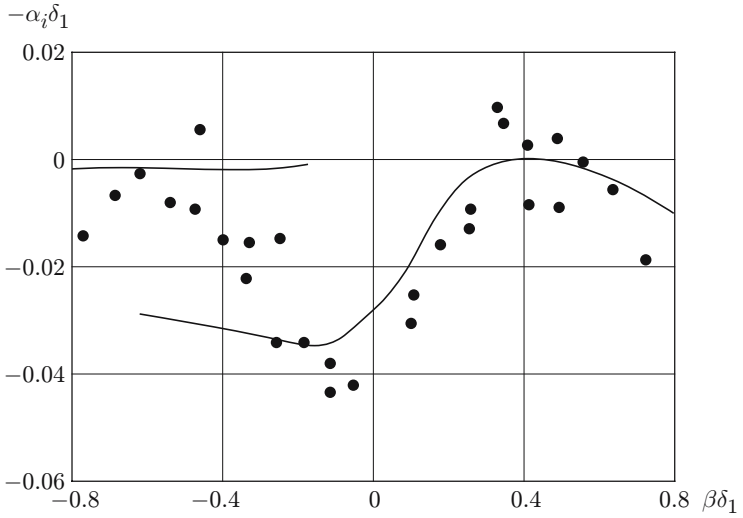

Fig. 4. Spatial growth rates of crossflow instability modes versus the spanwise wavenumber in the local coordinate system ($f = 35$ Hz): the curves refer to the the calculated data and the points refer to the measured data.

Quasi-two-dimensional waves (at $\beta \approx 0$) are strongly decaying. The most unstable modes are observed in narrow ranges of disturbance-propagation angles close to $\pm 90^\circ$ ($\beta\delta_1 \approx \pm 0.4$). The characteristic width of these regions decreases with decreasing frequency. In the range of negative spanwise wavenumbers, there is an interval $-0.6 < \beta\delta_1 < -0.2$, where the solution is not unique. Figure 4 displays two modes of the discrete spectrum, with one mode decaying much faster than the other. This phenomenon can be attributed to the fact that the mode with larger damping rates for $\beta < 0$ is the Tollmien–Schlichting instability mode. This assumption is confirmed by the computed value of its phase velocity $c = \omega/\alpha_r \approx 0.3$ (for $\beta = 0$) typical of the instability of this type. In the flow considered, however, this instability is suppressed by a sufficiently strong streamwise pressure gradient. The corresponding waves rapidly decay as they move downstream. In the above-mentioned range of the values of β, the points corresponding to the measured growth rates are located between two calculated curves. This allows us to assume that the sources of disturbances used in the experiments [11] generated disturbances of two types simultaneously, and the hot-wire anemometer recorded their combination.

The dispersion functions $\alpha_r = \alpha_r(\beta)$ obtained in the experiments and calculations are in good agreement for all frequencies [15].

2.3. Simulation of Test Conditions in the Supersonic Flow Regime. One objective of the present work was to simulate the experiments [9, 10]. The measurements were performed in a T-325 low-noise supersonic wind tunnel based at the Khristianovich Institute of Theoretical and Applied Mechanics of the Siberian Division of the Russian Academy of Sciences at a free-stream Mach number $M_\infty = 2$ and a Reynolds number per meter $Re_1 = 6.6 \cdot 10^6$ m^{-1}. A swept wing model with a symmetric profile and a leading-edge sweep angle $\lambda = 40^\circ$ was used. The model was mounted at a zero angle of attack. Controlled (artificial) disturbances were excited in the boundary layer on the model by a spark discharge point source [9]. The discharge ignition frequency was 10, 20, and 30 kHz. The mass-flux fluctuations were recorded by a constant-temperature anemometer. Frequency-wave amplitude-phase spectra of disturbances in several cross sections along the streamwise coordinate s were obtained by applying a discrete Fourier transform. The evolution of disturbances at the excited frequencies was found to be similar to the evolution of traveling waves at subsonic flow velocities. The results calculated by the linear stability theory are compared with experimental data below.

In the present work, the characteristics of the inviscid external flow were calculated by the formulas for the Prandtl–Meyer flow [16]. By virtue of a continuous isentropic expansion on the wing with a lenticular profile, the flow is accelerated, and the calculated local Mach number increases from $M_e \approx 1.6$ at $s = 0$ to $M_e \approx 2.36$ on the trailing edge of the wing at $s/c = 1$. The local sweep angle decreases continuously from $\lambda \approx 47^\circ$ to $\lambda \approx 36^\circ$, and the Hartree parameter increases from $\beta_H = 0$ to $\beta_H = 0.74$. The boundary layer on the model was calculated on

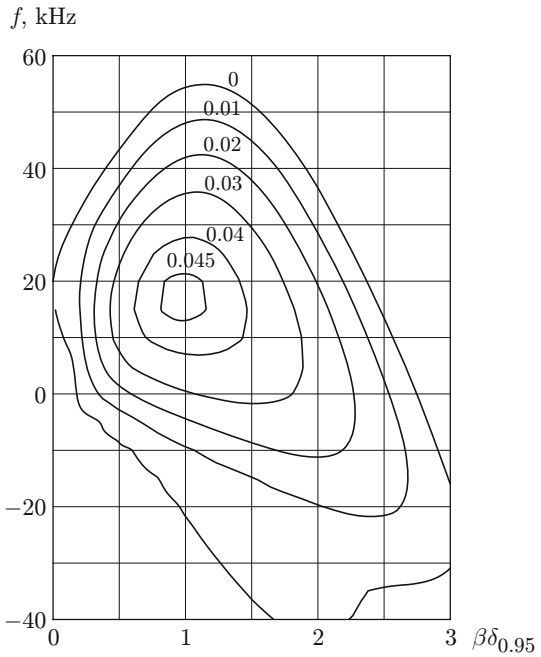

Fig. 5. Contours of spatial growth rates of disturbances $-\alpha_i\delta_{0.95}$ on the plane (β, f) in the local coordinate system at $x/c \approx 0.375$.

the basis of the distributions $\lambda(s)$, $\beta_H(s)$, and $\mathrm{M}_e(s)$ in the approximation of local self-similarity. It turned out that the absolute values of $W_{\max}$ increase from zero at the wing leading edg to $|W_{\max}| \approx 0.12$ at the trailing edge.

The linear stability of the three-dimensional boundary layer on the swept wing model under study showed that the instability region begins close to the leading edge of the model ($s/c \approx 0.06$). The growth rates of stationary modes continuously increase in the downstream direction until the trailing edge.

Figure 5 shows the theoretical stability diagram for the examined flow: contours of spatial growth rates on the plane (β, f) at $x/c \approx 0.375$ ($s = 75$ mm), i.e., in the region of growth of natural fluctuations. The region of negative values of frequency on this diagram corresponds to waves propagating in the secondary flow direction. The greatest growth rates in this cross section s are seen to correspond to traveling waves with a frequency $f \approx 20$ kHz and $\beta\delta_{0.95} \approx 1$; the values $-\alpha_i\delta_{0.95}$ are greater than the maximum growth rate of disturbances of stationary modes ($f = 0$) by a factor of 1.5. The range of frequencies with increasing disturbances propagating in the direction opposite to the secondary flow ($\beta > 0$) is $0 \leqslant f < 55$ kHz, which is in qualitative agreement with the experimental results [10], where amplification of natural background fluctuations with frequencies 5 kHz $\leqslant f <$ 40 kHz was observed.

The calculated and measured spatial growth rates are plotted in Fig. 6. The experimental points were obtained by means of differentiation of the measured spectra of natural disturbances of the boundary layer on the swept wing model over the streamwise coordinate (see Fig. 2a in [10]), while the theoretical curve was constructed over the maximum values $-\alpha_{i,\max}(f) = \max\limits_{\beta}[-\alpha_i(f,\beta)]$ determined from the stability diagram (see Fig. 5). The theoretical and experimental data are seen to agree well at high frequencies (15 kHz $\leqslant f <$ 50 kHz). At low frequencies ($f <$ 15 kHz), the measured growth rates are substantially smaller. A possible reason is the dominating contribution of external acoustic disturbances (wind-tunnel noise) into the low-frequency part of the spectrum; the intensity of these acoustic disturbances depends weakly on the streamwise coordinate, and their growth rates are small.

Figure 7 shows the dispersion curves $\alpha^* = \alpha^*(\beta^*)$ calculated in the coordinate system (s, z^*) for different frequencies. In the examined range of parameters, the theoretical and experimental [10] data are in good agreement.

For comparisons of the spatial growth rates of normal crossflow instability modes, we used the measured spectra of artificial disturbances (see Fig. 4 in [10]). Figure 8 shows the growth rate of disturbances as a function

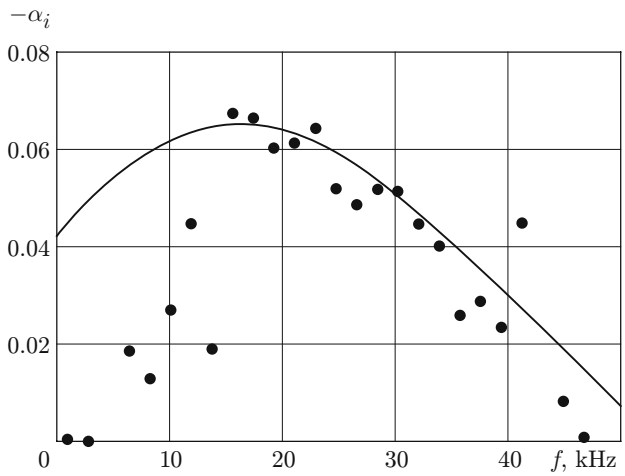

Fig. 6. Spatial growth rates of the spectral components of natural disturbances: the curve and the points refer to the calculated results and the experimental data [10], respectively.

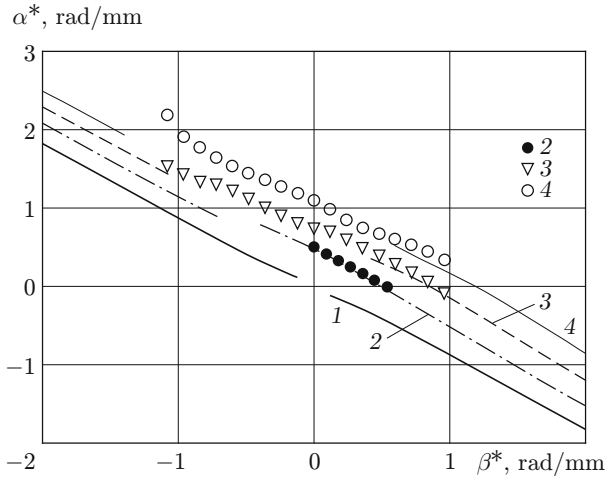

Fig. 7

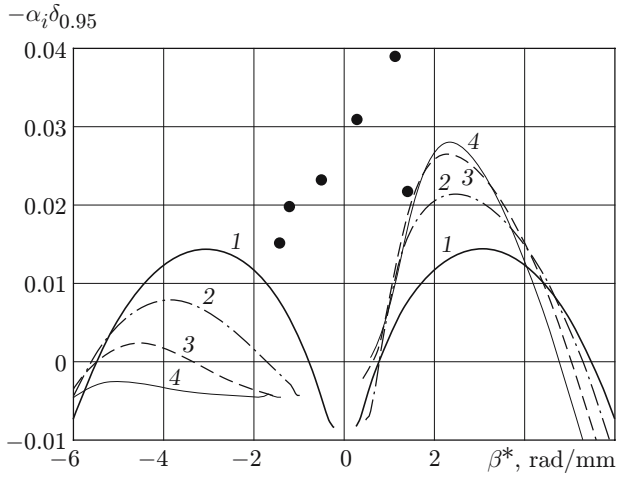

Fig. 8

Fig. 7. Streamwise wavenumber of normal instability modes versus the spanwise wavenumber in the coordinate system fitted to the leading edge of the model: the curves and the points refer to the calculated data and the experimental results [10], respectively, for $f = 0$ (1), 10 (2), 20 (3), and 30 kHz (4).

Fig. 8. Spatial growth rates of disturbances versus β^* in the wing-fitted coordinate system (s, z^*) at $s = 30$ mm: the curves are the calculated data for $f = 0$ (1), 10 (2), 20 (3), and 30 kHz (4); the points are the experimental data [10] for $f = 10$ kHz.

of the spanwise wavenumber at $s = 30$ mm. In contrast to the dispersion dependences, the theoretical results here do not agree with the experimental data. In the experiments, the fastest growth of disturbances is observed in the region 0.3 rad/mm $< \beta^* <$ 1.2 rad/mm, while the linear theory predicts the maximum growth of disturbances in the interval 2 rad/mm $< \beta^* <$ 3 rad/mm. The measured values of $-\alpha_i\delta_{0.95}$ are significantly higher than the calculated results.

Such a discrepancy between the calculated and experimental data is, apparently, explained by the initial conditions imposed in the experiment. In the experiments [9, 10], the amplitude of the mass flux of disturbances reached 30% of the mean value. A substantial distortion of the mean flow in the boundary layer was observed,

which suggests that the field of disturbances is nonlinear. Hence, the area of applicability of the linear theory for modeling such a process is rather limited. In addition, the range of the initial (in terms of the coordinate z^*) disturbance was rather large in the experiments, i.e., waves with low values of β^* dominated in the wave spectrum of the initial disturbances at the generation frequency. It was the growth of these disturbances that was registered in the downstream direction.

There seem to be some other reasons for the dominating growth of modes with $\beta^* \approx 0$. The experiments [17] performed in a two-dimensional boundary layer on a flat plate at M = 2 and higher intensities of initial disturbances also revealed the predominant growth of two-dimensional fluctuations, whereas it is three-dimensional linear disturbances that increase most rapidly in a supersonic boundary layer. This fact was explained in [18], where the evolution of disturbances of higher intensities in a supersonic boundary layer was demonstrated to be determined by the presence of stationary disturbances responsible for the mean field distortion. As a result, two-dimensional components of the disturbance spectrum are mainly amplified. Apparently, the higher initial amplitude of cross-flow instability modes excited in a three-dimensional boundary layer on a swept wing in the experiments [10] also produces the mean flow distortion, and the measured stability characteristics of such a flow deviate from those calculated by the linear theory.

Thus, the calculated spanwise scales of secondary flow disturbances are demonstrated to agree well with experimental data on stability of a three-dimensional supersonic boundary layer with artificial disturbances at M = 2. The calculated growth rates of disturbances, however, differ from the measured values. At the same time, the linear stability theory offers an adequate description of the development of natural disturbances whose amplitudes are much lower than the amplitudes of artificial disturbances.

This work was supported by the Russian Foundation for Basic Research (Grant No. 05-01-00079-a).

REFERENCES

1. V. N. Zhigulev and A. M. Tumin, *Origination of Turbulence* [in Russian], Nauka, Novosibirsk (1987).
2. H. L. Reed and W. S. Saric, "Stability of three-dimensional boundary layers," *Ann. Rev. Fluid Mech.*, **21**, 235–284 (1989).
3. W. S. Saric, H. L. Reed, and E. B. White, "Stability and transition of three-dimensional boundary layers," *Annu. Rev. Fluid Mech.*, **35**, 413–440 (2003).
4. S. G. Lekoudis, "Stability of three-dimensional compressible boundary layers over wings with suction," AIAA Paper No. 79-0265 (1979).
5. L. M. Mack, "Compressible boundary layer stability calculations for sweptback wings with suction," *AIAA J.*, **20**, No. 3, 363–369 (1982).
6. Yu. G. Ermolaev, A. D. Kosinov, V. Ya. Levchenko, and N. V. Semionov, "Instability of a three-dimensional supersonic boundary layer," *J. Appl. Mech. Tech. Phys.*, **36**, No. 6, 840–843 (1995).
7. H. L. Reed and W. S. Saric, "Control of transition in supersonic boundary layers using distributed roughness — experiments and computations," in: *Proc. West East High Speed Flow Fields* (Marseille, France, April 22–26, 2002), CIMNE, Barselona (2003), pp. 417–425.
8. N. V. Semionov, A. D. Kosinov, and V. Ya. Levchenko, "Experimental study of turbulence beginning and transition control in a supersonic boundary layer on swept wing," in: *Laminar–Turbulent Transition*, Proc. of the 6th IUTAM Symp. (Bangalore, India, December 13–17, 2004), Springer, New York (2006), pp. 355–362.
9. A. D. Kosinov, N. V. Semionov, Yu. G. Ermolaev, and V. Ya. Levchenko, "Experimental study of evolution of disturbances in a supersonic boundary layer on a swept-wing model under controlled conditions," *J. Appl. Mech. Tech. Phys.*, **41**, No. 1, 44–49 (2000).
10. N. V. Semionov, A. D. Kosinov, and V. Ya. Levchenko, "Experimental study of disturbance development in a 3D supersonic boundary layer," in: *Proc. West East High Speed Flow Fields* (Marseille, France, April 22–26, 2002), CIMNE, Barselona (2003), pp. 426–433.
11. V. R. Gaponenko, A. V. Ivanov, and Y. S. Kachanov, "Experimental study of stability of the boundary layer on a swept wing to nonstationary disturbances," *Teplofiz. Aéromekh.*, **2**, No. 4, 333–359 (1995).
12. M. Asai, N. Saitoh, and N. Itoh, "Instability of compressible three-dimensional boundary layer to stationary disturbances," *Trans. Japan Soc. Aeronaut. Space Sci.*, **43**, No. 142, 190–195 (2001).

13. S. A. Gaponov and A. A. Maslov, *Development of Disturbances in Compressible Flows* [in Russian], Nauka, Novosibirsk (1980).
14. W. D. Hayes and R. F. Probstein, *Hypersonic Flow Theory*, Academic Press, New York (1959).
15. S. A. Gaponov and B. V. Smorodskii, "Linear stability of a supersonic boundary layer on a swept wing," in: *High-Velocity Hydrodynamics and Numerical Modeling*, Proc. 3rd Int. Summer Scientific School (Kemerovo, Russia, June 22–28, 2006), Izd. Kemer. Univ., Kemerovo (2006), pp. 253–261.
16. J. D. Anderson, *Modern Compressible Flow*, McGraw-Hill, New York (1990).
17. A. D. Kosinov, Yu. G. Ermolaev, and N. V. Semionov, " 'Anomalous' nonlinear wave phenomena in a supersonic boundary layer," *J. Appl. Mech. Tech. Phys.*, **40**, No. 5, 858–864 (1999).
18. S. A. Gaponov and N. M. Terekhova, "Evolution of disturbances of elevated intensity in a supersonic boundary layer," *Aéromekh. Gaz. Dinamika*, No. 1, 28–36 (2003).